

Relativistic Effects on Metal–Metal Bonding: Comparison of the Performance of ECP and Scalar DKH Description on the Picture of Metal–Metal Bonding in $\text{Re}_2\text{Cl}_8^{2-}$

Robert Ponec,^{*,†} Lukáš Bučinský,[‡] and Carlo Gatti[§]

Institute of Chemical Process Fundamentals, Academy of Sciences of the Czech Republic v.v.i., Prague 6, Suchbát 2, 165 02 Czech Republic, Institute of Physical Chemistry and Chemical Physics, Slovak University of Technology in Bratislava, Bratislava, Slovakia, and Istituto di Scienze e Tecnologie Molecolari del CNR (CNR-ISTM) e Dipartimento di Chimica Fisica ed Elettrochimica, Università di Milano, Via Golgi 19, I-20133, Milano, Italy

Received June 21, 2010

Abstract: This paper reports a systematic comparison of the performance of alternative methods of including relativistic effects on the nature of metal–metal bonding in the $\text{Re}_2\text{Cl}_8^{2-}$ anion. The comparison involved the description using a scalar relativistic Douglas–Kroll–Hess (DKH2) Hamiltonian with all-electron basis sets and the relativistic effective core potential (ECP) basis sets. The impact of the above methods on the picture of the bonding was analyzed using the so-called domain averaged Fermi holes (DAFH). Besides comparing the impact on the picture of the bonding of the two above methods, the focus was also put on the systematic comparison of the “exact” AIM generalized form of DAFH analysis with the approximate Mulliken-like approach used in an earlier DAFH study of ReRe bonding. It has been shown that in contrast to descriptions using ECP basis sets where the differences in the picture of the bonding emerging from the approximate and “exact” DAFH analysis are only marginal, the approximate DAFH approach has been found to dramatically fail in the case of all-electron basis sets required for the description in terms of the Douglas–Kroll–Hess (DKH2) Hamiltonian.

Introduction

Since its discovery in the early 1960s, the chemistry of molecules involving direct metal–metal bonds has been the subject of growing interest. The motivation for these studies not only originated from the new perspectives that the existence of molecules with metal–metal bonds opened for the synthesis of new molecules and materials but, of the same or comparable importance, the challenge was also for the chemical theory to explain often unusual multiplicities of metal–metal bonds. One of the important factors undoubtedly contributing to the peculiarity of metal–metal bonds, especially among heavy transition metals such as Re, is the

relativistic effects.^{1–4} An example in this respect can be, e.g., the contraction of atomic radii of heavier metals often referred to as lanthanoid or actinoid contraction^{5,6} and the great enhancement of the so-called inert-pair effect,⁷ which is the main cause of the specificities in the chemistry of gold and mercury,^{7–10} and an inherently relativistic effect is also spin–orbit coupling. Because of the important impact of these effects on various observable molecular properties like bond lengths, bond energies, valency changes, magnetic properties, etc., the correct description of heavy atom chemistry requires taking the relativistic phenomena into account. The most general formulation of the relativistic quantum theory of free electron is provided by the four-component Dirac equation.¹¹ Despite considerable progress in the formulation of the procedures providing the solution at this fundamental level,¹² the application of such approaches is still considerably time-consuming and, if pursued,

* Corresponding author e-mail: rponec@icpf.cas.cz.

[†] Academy of Sciences of the Czech Republic v.v.i.

[‡] Slovak University of Technology in Bratislava.

[§] CNR-ISTM-Università di Milano.

would lead to lengthy and complex calculations. For that reason, and because of the importance of a reliable description of relativistic effects for bigger molecules of real chemical interest, various approximate quasi-relativistic approaches were proposed in past years with the aim to avoid the complexity of the four-component Dirac theory without a sacrifice of the accuracy. An example in this respect can be, e.g., explicit inclusion of relativistic effects via the Douglas–Kroll–Hess Hamiltonian,^{13,15} but widespread use has found also another conceptually different approach based on the use of effective core potentials.^{16–20}

The increasing interest in the detailed scrutiny of relativistic effects on the electron structure of molecules with heavy transition metals and/or actinides finds its manifestations, e.g., in the studies given in refs 21–30.

Our aim in this study is to report the detailed comparison of the performance of the above two types of approaches for the description of the picture of the bonding of multiple metal–metal bonds in $\text{Re}_2\text{Cl}_8^{2-}$. Because of the prominent position of this ion as a paradigm for quadruple metal–metal bonding, the nature of the Re–Re bond has been the subject of numerous studies.^{31–43} Into the framework of these efforts can also be included our recent study in which the nature of Re–Re bonding was discussed using the methodology known as the analysis of domain averaged Fermi holes.⁴⁰ Its conclusions were completely consistent with the results of other theoretical studies, according to which one of the four shared electron pairs involved in the bonding is considerably weaker than the remaining three so that the bond can be best classified as an *effective* triple bond. The analysis was performed in the study⁴⁰ using the approximate Mulliken-like approach, and the relativistic effects were included via the effective core potentials at the B3LYP/LANL2DZ level of the theory. In this report, we are going to extend the original study through a detailed comparison that involves (i) the eventual impact on the picture of the bonding of the alternative inclusion of the relativistic effects via the Douglas–Kroll–Hess Hamiltonian and all-electron basis sets and (ii) a detailed inspection of the picture of the bonding resulting from the approximate Mulliken-like and “exact” AIM generalized form of DAFH analysis so as to reveal any eventual bias resulting from the original use of the approximate Mulliken-like approach.

Theoretical

The DAFH analysis was proposed some time ago^{44–46} as a new tool for the description and visualization of the bonding interactions, and its recent applications in the realm of metal–metal bonding^{47–50} have provided new insights revealing the peculiarities of this widely studied type of bonds. Because most of such bonds, especially among heavier metals, can undoubtedly be affected by the operation of relativistic effects, we decided in this study to focus on just to what extent the picture of the metal–metal bonding can be sensitive to various methods of including relativistic effects in a quantum chemical description. Although the formalism of DAFH analysis was repeatedly described in earlier studies, we consider it useful to review the basic ideas of the approach and, also, to incorporate the original

intuitively formulated formalism into the language of a strict, more elegant, mathematical description.

The original introduction of domain averaged Fermi holes, $g_\Omega(r)$, referred to the concept of the correlation hole,⁵¹ from which the corresponding holes are derived by the selective integration over the coordinates of one electron of the pair, as suggested in eq 1.

$$\begin{aligned} C(r, r') &= 2\rho(r, r') - \rho(r)\rho(r') \\ g_\Omega(r) &= - \int_\Omega C(r, r') \, dr' = \rho(r) \int_\Omega \rho(r') \, dr' - \\ &\quad 2 \int_\Omega \rho(r, r') \, dr' \end{aligned} \quad (1)$$

where $\rho(r)$ and $\rho(r, r')$ denote ordinary one-electron and pair density, respectively, and the integration is over the finite domain Ω . For the sake of mathematical elegance, it is possible to reformulate the whole approach in terms of density matrices rather than densities, although the specific choice of either formulation has no impact on the practical applicability of the DAFH analysis. For this purpose, let us introduce first the exchange-correlation density matrix (eq 2)

$$\rho^{\text{exc}}(r_1, r_1'; r_2, r_2') = \rho(r_1, r_1')\rho(r_2, r_2') - 2\rho^{(2)}(r_1, r_1'; r_2, r_2') \quad (2)$$

which measures the deviation of two electrons from independent electron behavior to truly correlated behavior via one-electron density matrices $\rho(r_1, r_1')$ and $\rho(r_2, r_2')$ and the two-electron density matrix $\rho^{(2)}(r_1, r_1'; r_2, r_2')$. On the basis of eq 2, it is possible to introduce the domain averaged Fermi-hole matrix $g_\Omega(r_1, r_1')$ by the selective integration of the matrix (eq 2) over the finite domain Ω .

$$g_\Omega(r_1, r_1') = \int_{r_2=r_2'; \Omega} \rho^{\text{exc}}(r_1, r_1'; r_2, r_2') \, dr_2 \quad (3)$$

Although the choice of the domain is in principle arbitrary and the corresponding Fermi hole densities and/or holes can be averaged over domains of arbitrary shape and size, in previous studies, we have demonstrated that especially interesting and chemically relevant information can be extracted from these holes if the integration domains coincide with AIM atomic domains resulting from the virial partitioning of electron density.⁵² Constructed and analyzed can be, however, also more complex domains formed by union of several atomic domains corresponding to, e.g., various functional groups or interesting molecular fragments. In such a case, the holes provide the information about the electron pairs retained in the domain as well as about broken or dangling valences created by the formal splitting of the bonds required for the isolation of the domain from the rest of the molecule. The DAFH analysis involves, as a first step, the diagonalization of the matrix representing the Fermi hole density in an appropriate basis. The eigenvectors and eigenvalues resulting from such a diagonalization are then, in the second step, subjected to the so-called isopycnic transformation,⁵³ whose aim is to transform the original eigenvectors to more localized functions that provide an appealing and highly visual description of the molecular structure in terms close to classical chemical thinking. The

structural information is primarily extracted from the resulting eigenvalues which allow detection of electron pairs (chemical bonds, core and lone pairs) retained in the domain as well as broken or dangling valences formed by the formal splitting of the bonds required for the isolation of the domain from the rest of the molecule. The above interpretation is then significantly facilitated by the graphical display of the eigenvectors associated with the corresponding eigenvalues.

Although the definition of DAFH is completely general and can be applied at any level of the theory, most of the previous applications in the realm of metal–metal bonding^{47–50} have been performed using several simplifying approximations.

The first of them concerns the pair density. The extraction of this density from post-Hartree–Fock calculations is not an easy task, and the use of DAFH analysis at a correlated level of the theory has been reported only recently and for small systems.^{54,55} For the complexes of transition metals, such an approach is still beyond the reach of present possibilities. Much more feasible is the approach based on the Kohn–Sham DFT level of the theory,^{56,57} which, especially in inorganic chemistry, represents the contemporary computational standard. In such a case, the general definition of the DAFH (eq 1) reduces to

$$g_{\Omega}(r_1, r_1') = 2 \sum_i^{\text{occ}} \sum_j^{\text{occ}} \langle ij | \rangle_{\Omega} \varphi_i(r_1) \varphi_j(r_1') \quad (4)$$

where

$$\langle ij | \rangle_{\Omega} = \int_{\Omega} \varphi_i(r_2) \varphi_j(r_2) dr_2 \quad (5)$$

denotes the overlap integral of molecular orbitals i and j over the domain Ω . Formula 4 results from the general definition (eq 1) if the pair density is formally constructed from the first-order density matrix using the formula exactly valid at one-determinantal Hartree–Fock level. Its use at the DFT level of theory, which provides only the first-order density and not the density matrix, thus certainly represents a kind of heuristic extension, but the results of earlier applications of this approach to other systems with metal–metal bonds provide a clear justification for the reliability of the picture of the bonding in such systems.^{47–50} This is also true for an earlier study of Re–Re bonding,⁴⁰ where, consistent with the results of recent sophisticated CASSCF calculations,^{37,39} the analysis detected the reduction of Re–Re bond multiplicity resulting from the partial population of the antibonding δ^* orbital. This result thus in a sense confirms the conclusions of the recent study by Truhlar et al.,⁵⁸ which claims that the use of density-based exchange functionals may provide a more theoretically justified way to treat transition metals than post-Hartree–Fock wave function methods and not just a cost-effective alternative to wave-function-based methods.

The second approximation which was often used in our earlier DAFH studies of transition metal systems concerned the simplification of replacing the exact integration over AIM domains by the Mulliken-like approximation, according to which the electron is in the domain of atom A if it is in the orbital attached to that atom. The simplest implementation

of such an approximate DAFH analysis is based on a simplification of formula 5 for the elements of the AOM matrix due to a transformation to a symmetrically orthogonalized AO basis

$$\mathbf{o} = \mathbf{S}^{1/2} \mathbf{c} \quad (6)$$

In such a case, the elements of the AOM matrix associated with atom A can be written as

$$\langle ij | \rangle_A = \sum_{\mu} \sum_{\nu} c_{\mu i} c_{\nu j} S_{\mu\nu}^A \rightarrow \sum_{\mu} o_{\mu i} o_{\mu j} \quad (7)$$

so that the attachment of (orthogonalized) basis functions to atoms is straightforward. Using the orthogonalized AO basis, the elements of the \mathbf{g} matrix (eq 4) can be written as

$$\mathbf{G}_{\lambda\sigma}^A = \frac{1}{2} \sum_{\mu} \mathbf{D}_{\mu\lambda} \mathbf{D}_{\mu\sigma} \quad (8)$$

where \mathbf{D} , given by eq 9,

$$\mathbf{D} = \mathbf{S}^{1/2} \mathbf{P} \mathbf{S}^{1/2} \quad (9)$$

is the first-order density matrix in the orthogonalized AO basis. For the purpose of graphical display, the resulting localized eigenvectors have to be, of course, back-transformed into the original nonorthogonal basis.

The reason for the use of this approximation was that in early studies on metal–metal bonding,^{47–50} the transition metals were described using relativistic ECP basis sets, which are known to produce densities whose integration is not always straightforward.^{59–61} As we are now able to overcome the above numerical problems, the possibility to use the DAFH analysis at an exact AIM-generalized level of theory opens the way to a detailed study of the eventual bias resulting for the picture of Re–Re bonding from the use of an approximate Mulliken-like form of the approach.

In addition to this, the availability of the exact AIM generalized form of the analysis also opens the possibility for the direct comparison of the performance of various methods of inclusion of relativistic effects on the picture of the Re–Re bonding. Recently, such a comparison between the exact AIM-generalized level and the approximate Mulliken form of the DAFH analysis has been performed for two prototypical systems (homoleptic binuclear metal carbonyls) for which the 18-electron rule predicted the existence of a direct metal–metal bond. As it has been shown, the picture of the bonding provided by both forms of DAFH analysis is remarkably consistent and clearly indicates that residual bonding interactions between metals originate from multicenter bonding involving bridging ligands.⁶²

For the sake of straightforward comparison with an earlier study,⁴⁰ we focus here on the description of relativistic effects via ECP basis set LANL2DZ¹⁸ and the scalar relativistic DKH2 approach using the all-electron VTZ basis.⁶³ Such a comparison is performed for the fixed molecular geometry used in the study,⁴⁰ which resulted from the optimization at the B3LYP/LANL2DZ level of theory and which closely reproduced the experimental geometry. In addition to this, we also present a comparison of geometry optimization using

Table 1. Comparison of Experimental and Calculated (B3LYP/LANL2DZ) Geometrical Parameters of the $\text{Re}_2\text{Cl}_8^{2-}$ Ion

geometrical parameters	calculated (bond lengths in pm, angles in deg)	experimental (bond lengths in pm, angles in deg)
R_{ReRe}	221	224 ⁷⁴ 222 ⁷⁵
R_{ReCl}	243	229 ⁷⁴ 243 ⁷⁵
$\angle\text{ReReCl}$	105	104 ⁷⁴ 104 ⁷⁵

the relativistic one-component (scalar) DKH2, two-component DKH2, and nonrelativistic description in all-electron uncontracted DZ basis^{63,64} to see to what extent the inclusion and/or omission of relativistic effects and spin–orbit interactions can affect the geometrical structure of the $\text{Re}_2\text{Cl}_8^{2-}$ ion.

Computations

The application of DAFH analysis requires to perform several types of calculations. First, it is necessary to generate the wave function using ordinary quantum chemical methods. In this study, these calculations were performed for the fixed geometry of the ion generated for the purpose of an earlier DAFH study on the bonding in the $\text{Re}_2\text{Cl}_8^{2-}$ anion⁴⁰ by the geometry optimization at the B3LYP/LANL2DZ level of the theory. The comparison of calculated geometrical parameters with the experimental data is summarized in Table 1. For the sake of a straightforward comparison of the eventual impact on the picture of the bonding of various methods of including the relativistic effects, the wave functions were generated using (i) a relativistic ECP basis set at the B3LYP/LANL2DZ level of the theory and (ii) a scalar relativistic DKH2 approach using the all-electron VTZ basis sets spanned for the Re atom by the Foldy–Wouthuysen recontracted TZ basis set of Dyall⁶³ and for the Cl atom by the Douglas–Kroll recontracted cc-VTZ basis set.^{64,65} Moreover, the Re TZ basis set of Dyall⁶³ has been extended by valence correlating functions⁵⁰ with the final contraction scheme (29s24p15d11f)→[8s7p6d4f]. On the basis of this primary wave function generated by Gaussian 03,⁶⁶ the second step involves the generation of AOM matrices required, according to eq 2, for the generation of the DAFH. These calculations were performed using the PROAIM and AIMAll programs.^{67,68} After having generated the AOM matrices, the last step consists of the generation and subsequent analysis of the DAFH (eq 1), using our program WinBader, which is available upon request. In the following part, the results of these analyses are reported. In addition to the detailed study of the eventual impact on the picture of the bonding of various alternative methods of inclusion of relativistic effects for the fixed geometry of the $\text{Re}_2\text{Cl}_8^{2-}$ ion, we have also focused on the impact of the same methods on the optimized molecular geometry of the $\text{Re}_2\text{Cl}_8^{2-}$ ion. For this purpose, we performed a reoptimization of the geometry at the one-component (scalar) DKH2, two-component DKH2, and nonrelativistic B3LYP levels of the theory using the uncontracted DZ^{63,64} basis set. These calculations were performed

with the Dirac08 package.¹² At the DKH2 level, first-order methods have been used, and the resulting reoptimized geometries are summarized in Table 4.

Results and Discussion

Before pursuing the primary goal of this study, which is a comparison of the impact on the picture of the ReRe bonding of various procedures of inclusion of relativistic effects, we first briefly recall the results of the previous DAFH study in which the analysis of the bonding interactions was performed using an approximate Mulliken-like approach at the B3LYP/LANL2DZ level of the theory. Of decisive importance in this respect are the analyses of the DAFHs averaged over the fragments Re–Re and ReCl_4 . According to general interpretation, the DAFH analysis of the Fermi hole averaged over a certain fragment reveals the existence of electron pairs (chemical bonds, core or lone pairs) retained in the fragment as well as broken or dangling valences resulting from the formal splitting of the bonds required to isolate the fragment from the rest of the molecule. Thus, e.g., in the case of the hole averaged over the ReCl_4 fragment, one should see, besides electron pairs of inner shells on Re and lone pairs on Cl atoms, the existence of electron pairs of ReCl bonds as well as the broken or dangling valences whose number should indicate the number of broken ReRe bonding electron pairs, i.e., the multiplicity of the metal–metal bond. This information can then be independently checked by the analysis of the complementary hole averaged over the fragment ReRe, which directly detects the electron pairs involved in metal bonding. This implies that if the ReRe bond was indeed a quadruple bond, the information from both complementary analyses (for both the fragments ReRe and ReCl_4) should be consistent and indicate the presence of four bonding electron pairs as well as four broken valences. In the original study⁴⁰ based on the approximate Mulliken-like approach, such an ideal complementarity was not observed. Besides four bonding electron pairs (one σ , two π , and one δ) involved in ReRe bonding, the analysis detected in the same fragment the partial population of the antibonding δ^* orbital, whose contribution partly cancels the bonding contribution of the bonding δ orbital and thus reduces the effective multiplicity of the ReRe bond to 3. As, however, the above picture of the bonding resulted from the approximate Mulliken-like form of the analysis, it was of interest to see whether or to what extent the picture of the bonding could be affected if the approximate Mulliken-like DAFH analysis was replaced by the exact AIM-generalized description. In the following part, we are going to show that the differences between the approximate Mulliken-like and exact AIM-generalized description are both qualitatively and quantitatively only marginal for the analysis based on B3LYP/LANL2DZ calculations. The first indication of the close resemblance of the picture of the ReRe bonding comes already from the comparison of calculated ReRe bond orders characterized by Wiberg–Mayer bond indices^{69,70} and/or their AIM generalized counterparts.^{71,72} The actual values, equal to 2.836 and 2.690, respectively, are not only close numerically but the fact that both of them deviate significantly from the ideal value of 4 also indicates considerable

Table 2. Summary of Numerical Results of DAFH Analysis of the $\text{Re}_2\text{Cl}_8^{2-}$ Ion in Case of Relativistic Effects Included Using the ECP Basis Set

method	B3LYP/LANL2DZ				
	AIM		Mulliken		interpretation
	eigenvalue	degeneracy	eigenvalue	degeneracy	
ReCl ₄	≈ 2	4	≈ 2	4	inner shells on Re
	≈ 2	4	≈ 2	4	σ_{ReCl}
	≈ 2	12	≈ 2	12	lone pairs on Cl
	1.070	1	1.030	1	broken valence σ_{ReRe}
	1.035	2	1.060	2	broken valence π_{ReRe}
	1.091	1	1.13	1	broken valence δ_{ReRe}
ReRe	≈ 2	8	≈ 2	8	inner shells on Re
	1.96	1	1.99	1	σ_{ReRe}
	1.88	2	1.99	2	π_{ReRe}
	1.83	1	1.99	1	δ_{ReRe}
	0.435	1	0.63	1	δ^*_{ReRe}
	0.407	8	0.65	8	broken valence σ_{ReCl}

reduction of the multiplicity of the ReRe bond. In order to reveal the origin of this reduction as well as demonstrate the close resemblance of both descriptions, the results of both the exact AIM-generalized and Mulliken-like DAFH analyses for the fragments ReRe and ReCl₄ are summarized in Table 2 and in graphical form in Figures 1 and 2. Thus, e.g., the analysis of the hole averaged over the fragment ReCl₄ yields in both cases 24 nonzero eigenvalues of which 20 are very close to 2. The inspection of the corresponding eigenvalues shows that four of them correspond to electron pairs of inner *ns* and *np* shells on Re. Besides this, there are another 12 electron pairs corresponding to lone pairs on chlorine ligands

as well as four electron pairs involved in four ReCl σ bonds retained in the fragment (Figure 1d,h). What remains are the four eigenvalues close to 1, and the inspection of the associated eigenvectors shows that they indeed correspond to four broken valences (one σ , two π , and one δ component) of the ReRe bond (Figure 1a,e; b,f; c,g). These results are completely consistent with the quadruple multiplicity of the ReRe bond, and the close resemblance of the picture of the bonding is also clearly evident from Figure 1, which displays the comparison of selected eigenvectors resulting from both exact AIM-generalized and approximate Mulliken-like analyses for the fragment ReCl₄.

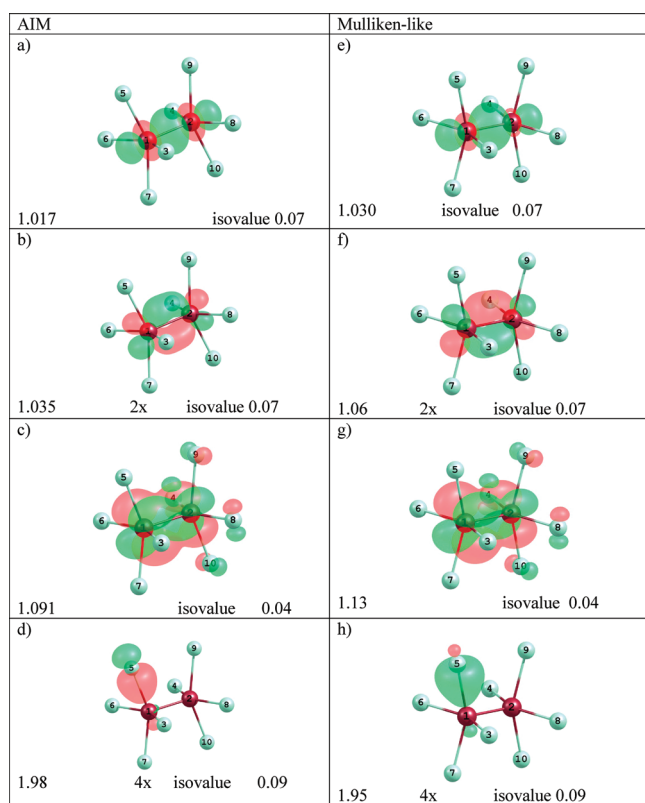
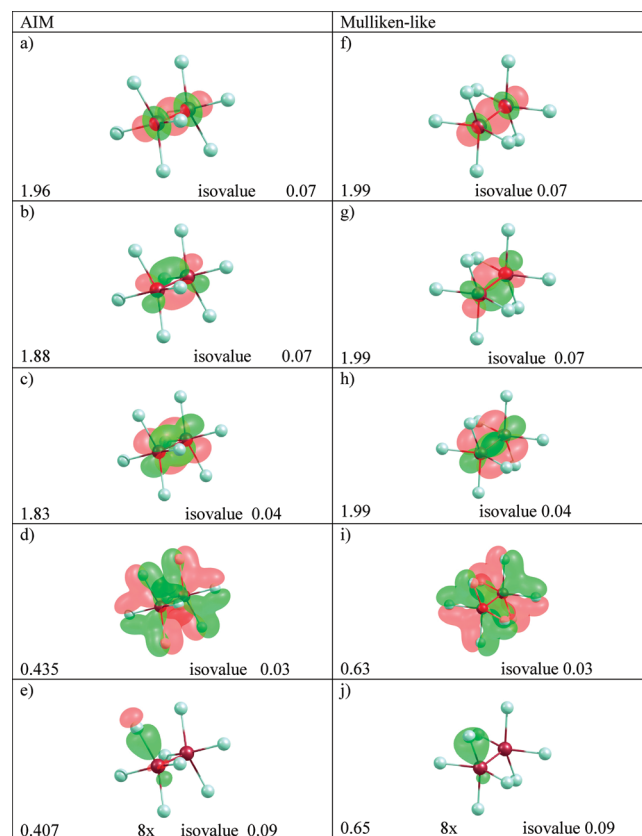
**Figure 1.** Comparison of selected eigenvectors resulting from the “exact” AIM generalized and approximate Mulliken-like DAFH analysis for the hole averaged at the B3LYP/LANL2DZ level of the theory over the fragment ReCl₄. [Pictures were generated using ChemCraft, v. 1.6.]**Figure 2.** Comparison of selected eigenvectors resulting from the “exact” AIM generalized and approximate Mulliken-like DAFH analysis for the hole averaged at the B3LYP/LANL2DZ level of the theory over the fragment ReRe.

Table 3. Summary of Numerical Results of the DAFH Analysis of the $\text{Re}_2\text{Cl}_8^{2-}$ Ion in the Case of Relativistic Effects Included via the DKH2 Level of Theory Using the Relativistic All Electron VTZ Basis Set

DKH2/VTZ					
base	AIM		Mulliken		
fragment	eigenvalue	degeneracy	eigenvalue	degeneracy	interpretation
ReCl4	≈ 2	20	≈ 2	20	inner shells on Cl atoms
	≈ 2	12	≈ 2	12	lone pairs on Cl atoms
	≈ 2	34	≈ 2	34	inner shells on Re
	1.98	4	1.91	4	σ_{ReCl}
	1.013	1	1.04	1	broken valence σ_{ReRe}
	1.035	2	1.05	2	broken valence π_{ReRe}
	1.08	1	1.09	1	broken valence δ_{ReRe}
ReRe	≈ 2	68	≈ 2	68	inner shells on Re
	1.93	1	1.98	1	σ_{ReRe}
	1.87	2	1.97	2	π_{ReRe}
	1.78	1	1.94	1	δ_{ReRe}
	0.39	1			δ^*_{ReRe}
	0.38	8	0.77	8	broken valence σ_{ReCl}
			0.23–0.40		20 weird eigenvectors

Similar close resemblance between the exact and approximate description is also observed for the analysis of the hole averaged over the complementary fragment ReRe. However, in contrast to the previous hole averaged over the fragment ReCl_4 whose analysis was straightforwardly consistent with quadruple multiplicity of the ReRe bond, an inspection of the results in this case indicates that the situation with metal–metal bonding is a bit more complex. The DAFH analysis of the hole averaged over the ReRe fragment yields, namely, in both cases, 21 nonzero eigenvalues, of which 12 are close to 2 and the remaining 9 vary between 0.41 and 0.65. The inspection of the eigenvectors corresponding to electron pairs shows that eight of them correspond to electron pairs of completely filled inner shells on Re atoms and as such are not involved in metal–metal bonding. What remains are four electron pairs associated with the remaining four eigenvalues close to 2, and the graphical inspection of these eigenvectors shows that they correspond to one σ , two π , and one δ component of the ReRe bond. As can be seen from the Figure 2 (Figure 2a vs f; b vs g; c vs h), the differences between the exact and approximated description are again very marginal. Although the existence of the above four bonding electron pairs is indeed consistent with the assumed quadruple multiplicity of the Re–Re bond, the problem with the above classification is that besides the above-mentioned four bonding electron pairs, the DAFH analysis again detected the existence of a partially populated δ^* orbital (Figure 2d vs i). This partially populated δ^* orbital corresponds to one of nine remaining eigenvectors, and it is associated with the eigenvalues 0.435 and/or 0.63 for the exact AIM generalized and approximate Mulliken-like description, respectively. Because the population of this antibonding δ^* orbital partially cancels the bonding contribution of the δ pair, the nature of Re–Re bond is again most consistent with a classification of an *effective* triple bond. The remaining eight partially populated eigenvectors correspond, as expected, to the broken valences of ReCl σ bonds (Figure 2e vs j). The differences in the corresponding eigenvalues (0.407 vs 0.65) only reflect the differences of AIM generalized and Mulliken-like descriptions in characterizing the uneven sharing of a bonding electron pair in the polar ReCl bond. On the basis of the above values, and consistent with known general trends, the polarity of the ReCl

bond estimated by the AIM generalized description exceeds the one from the approximate Mulliken-like approach.

After having demonstrated the close resemblance of the picture of the bonding based on the approximate Mulliken-like and “exact” AIM generalized form of the DAFH analysis in the case of relativistic effects included via the ECP basis set LANL2DZ, we are now going to scrutinize similarly the picture of the bonding resulting from the scalar relativistic DKH2 description using an all-electron VTZ basis.⁶³ The results of these analyses for the Fermi holes averaged over the fragments ReCl_4 and ReRe are summarized in Table 3 and Figures 3 and 4.

The simplest situation is again for the hole averaged over the fragment ReCl_4 where the analysis detects, besides others, the existence of four dangling valences corresponding to four formally broken electron pairs involved in ReRe bonding (Figure 3a vs e; b vs f; c vs g) as well as four electron pairs of localized ReCl σ bonds. (Figure 3d vs h). In this respect, the all-electron results are very similar to what was observed in the previous case using ECPs (Figure 1); the only difference is that because of using the all-electron basis set, the analysis now detects a much higher number (70) of eigenvalues close to 2, which correspond to completely filled inner shells on Re and Cl atoms.

The situation is, however, a bit more complex in the case of the hole averaged over the fragment ReRe. In this case, namely, the close resemblance to the results of previous analyses, using the LANL2DZ basis is observed only for the exact AIM-generalized approach, but for the approximate Mulliken-like approach, one observes clear differences that considerably question the reliability of Mulliken-like approach in the case of flexible all-electron relativistic basis sets. The first indication of possible inadequacy of the Mulliken-like approach is reflected already in the values of calculated ReRe bond orders [0.64 (Mulliken-like) vs 2.802 (AIM)]. While the value for the exact AIM generalized approach is not too much different from what was observed in the LANL2DZ basis, the Mulliken-like value is completely out of range of reasonable. The situation thus in a sense resembles the known failure of Mulliken population analysis for the extensive basis sets involving diffuse functions.⁷³

Besides the above differences, the possible inadequacy of the approximate Mulliken-like DAFH analysis using a

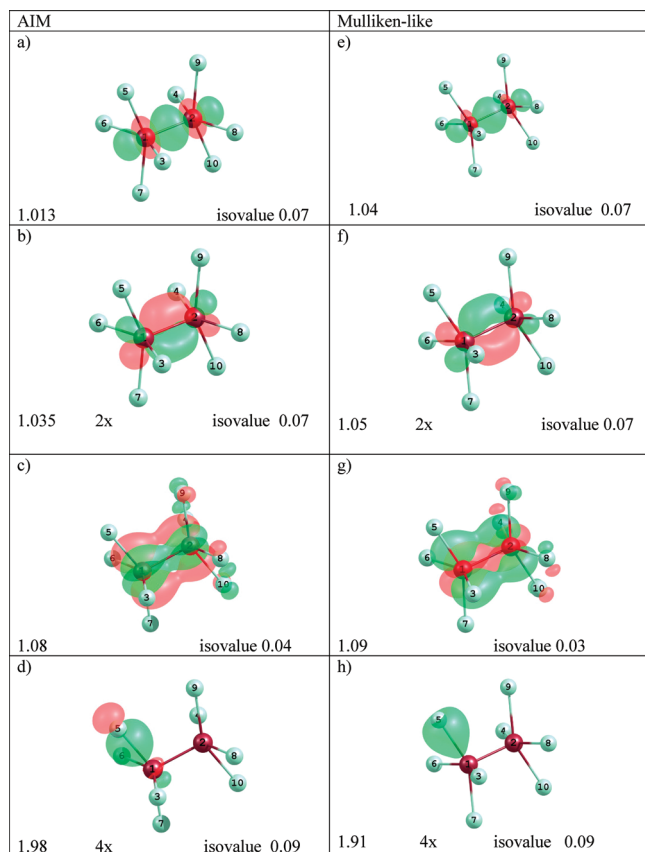


Figure 3. Comparison of selected eigenvectors resulting from the “exact” AIM generalized and approximate Mulliken-like DAFH analysis for the hole averaged at the DKH2/VTZ level of theory over the fragment ReCl_4 .

flexible relativistic all-electron basis set is also reflected in the important qualitative implications for the picture of the bonding emerging from the exact AIM generalized vs the approximate Mulliken-like form of DAFH analysis of the hole averaged over the fragment ReRe .

The results of such analyses, summarized in Table 3 and Figure 4, indicate that, while the AIM generalized approach detects, similarly as in the case of the ECP-based description, the existence of a partially populated antibonding δ^* orbital (Figure 4d), such an orbital is completely absent in the case of approximate Mulliken-like approach (Figure 4i). In addition to this, the Mulliken-like analysis also detects, however, the existence of a large number (20) of other weird eigenvectors with populations ranging between 0.23 and 0.40, whose contributions dramatically complicate a simple and transparent picture of the ReRe bonding.

This result is very important as it implies that the manifestations of relativistic effects on the picture of the ReRe bonding do not dramatically depend on the particular choice of the approach (scalar DKH2 description with all electron basis vs ECP basis) provided that the DAFH analysis is performed using the exact AIM-generalized approach. On the other hand, in the case of the approximate Mulliken-like form of the DAFH analysis, the reliable and internally consistent results are observed only in the case of relativistic effects included via small ECP basis sets, while in the case of the DKH2 description with relativistic all-electron basis sets, the use of the approximate Mulliken-like approach is

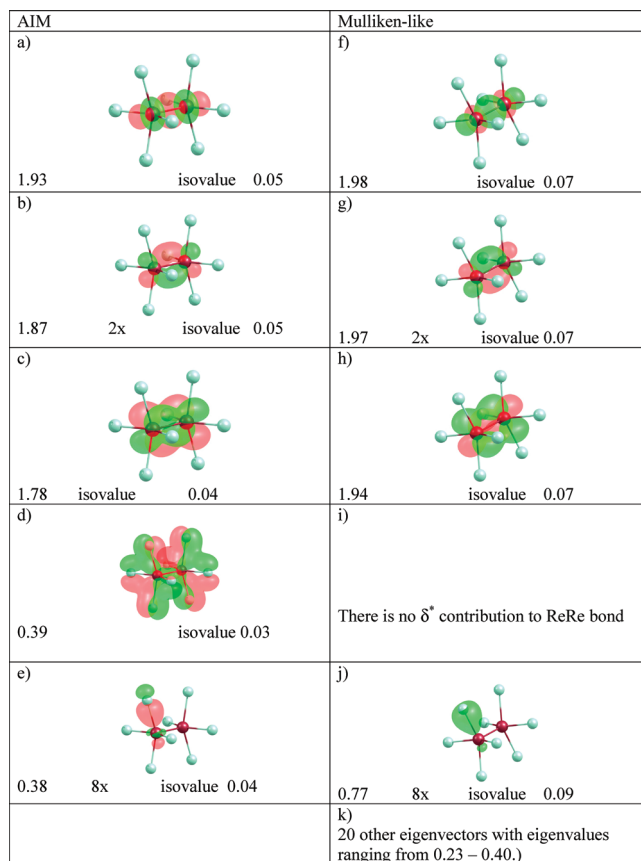


Figure 4. Comparison of selected eigenvectors resulting from the “exact” AIM generalized and approximate Mulliken-like DAFH analysis for the hole averaged at the DKH2/VTZ level of theory over the fragment ReRe .

questionable. In order to understand the reasons for the observed failure of Mulliken-like analysis for the flexible all-electron basis set, we have performed additional calculations using relativistic ECP LANL2TZ(f)^{18,76} for Re and the cc-pVTZ⁶⁴ basis for Cl, which explicitly contains one f function on Re. The results of both population and DAFH analysis in this basis are very reminiscent of the results in the LANL2DZ basis, which quite consistently keeps with the fact that the one f function in the ECP LANL2TZ(f) basis set is less diffuse, hence less “Mulliken-problematic”, than f functions in the all-electron VTZ basis.⁶³

After having presented the impact on the picture of the bonding of two alternative methods of including relativistic effects (AE-DKH2 vs ECP), we report, in the following part, the results of the systematic comparison of the effect of the same methods on the reoptimization of the molecular geometry of the $\text{Re}_2\text{Cl}_8^{2-}$ ion. The crucial geometrical parameters of the reoptimized structures are summarized in Table 4. As is possible to see from the comparison with the Table 1, the best agreement with the experimental geometry is obtained using the LANL2DZ ECP basis sets (for both Re and Cl). On the other hand, the geometry resulting from the optimization at the DKH2 level of theory using the all-electron basis set exhibits quite remarkable differences, and it is interesting that very similar structural parameters were obtained also using the LANL2TZ(f) ECP on Re and an AE cc-pVTZ basis set on the Cl atom (see Table 4)—a result

Table 4. Geometrical Parameters Resulting from the Optimization of the Molecular Geometry of the $\text{Re}_2\text{Cl}_8^{2-}$ Ion Using Various Methods of Inclusion of Relativistic Effects

method/basis	geometrical parameters	calculated values (bond lengths in pm, angles in deg)
nonrelativistic	R_{ReRe}	219.5
B3LYP/uncontractedDZ	R_{ReCl}	241.6
	$\angle\text{ReReCl}$	105.1
1c-DKH2	R_{ReRe}	219.2
B3LYP/uncontractedDZ	R_{ReCl}	237.4
	$\angle\text{ReReCl}$	104.9
2c-DKH2	R_{ReRe}	219.2
B3LYP/uncontractedDZ	R_{ReCl}	237.5
	$\angle\text{ReReCl}$	104.9
ECP-LANL2TZ ^a	R_{ReRe}	219.6
B3LYP/TZ	R_{ReCl}	236.0
	$\angle\text{ReReCl}$	104.9

^a Re, LANL2TZ(f); Cl, cc-pVTZ.

which raises some doubts on the physical significance of almost perfect matching between the experimental geometry and the theoretical prediction using the smaller basis set ECP model. Indeed, the geometry optimization with the LANL2DZ ECP might be influenced by error cancellations due to the fortunate combined effect of (a) the larger basis set superposition error (BSSE) inherent to a smaller basis set; (b) the specific contraction scheme of the original Hay and Wadt uncontracted Gaussian basis adopted in the LANL2DZ basis in contrast to the fully uncontracted scheme used for the LANL2TZ basis; and, finally, (c) the lack of the “f” polarization function in the LANL2DZ basis. A detailed and separate analysis of such effects, aimed at dissecting their specific role and relevance in determining the $\text{Re}_2\text{Cl}_8^{2-}$ geometry is, however, clearly outside the scope of the present paper.

Conclusions

This study reports a systematic comparison of the effect of various methods of inclusion of relativistic effects on the nature of metal–metal bonding in the $\text{Re}_2\text{Cl}_8^{2-}$ ion as reflected by the analysis of domain averaged Fermi holes. The comparison involved two widely used methods, namely, the approach based on the use of relativistic ECP basis sets and the direct Douglas–Kroll–Hess Hamiltonian using all-electron basis sets. It has been shown that the picture of the bonding emerging from both methods is practically insensitive to the actual method used provided the analysis is performed using the exact AIM-generalized form of the DAFH analysis and closely agrees with the results of earlier theoretical studies,^{32,34} according to which the partial cancellation of the bonding contribution of the δ bond due to fractional population of the antibonding δ^* orbital effectively reduces the multiplicity of the Re–Re bond, with the value close to 3. On the other hand, in the case of the approximate Mulliken-like approach of the DAFH analysis, the reliable and internally consistent results are observed only when relativistic effects are included via small ECP basis sets, while in the case of the DKH2 description with relativistic all-electron VTZ basis sets, the use of the approximate Mulliken-like approach seems questionable.

Acknowledgment. R.P. is thankful for the support of this study from the Grant Agency of the Czech Republic,

grant no. 203/118/09. The support from grants APVV (contract no. APVV-0093-07) and VEGA (contract nos. 1/0817/08 and 1/0127/09) is also gratefully acknowledged by L.B. Partial support from the Danish National Research Foundation through the Center for Materials Crystallography (CMC) is gratefully acknowledged by C.G.

References

- (1) Pitzer, K. S. *Acc. Chem. Res.* **1979**, *12*, 271–276.
- (2) Pyykkö, P. *Acc. Chem. res.* **1979**, *12*, 276–281.
- (3) Christiansen, P. A.; Ermler, W. C.; Pitzer, K. S. *Annu. Rev. Phys. Chem.* **1985**, *36*, 407–432.
- (4) Pyykkö, P. *Chem. Rev.* **1988**, *88*, 563–594.
- (5) Greenwood, N. N.; Earnshaw, A. *Chemistry of Elements*; Pergamon Press: Oxford, U. K., 1984; Chapter 30.
- (6) Seth, M.; Dolg, M.; Fulde, P.; Schwerdtfeger, P. *J. Am. Chem. Soc.* **1995**, *117*, 6597–6598.
- (7) Sidgwick, N. V. *The Covalent Link in Chemistry*; Cornell University Press: Ithaca, NY, 1933.
- (8) Wesendrup, R.; Laerdahl, J. K. *J. Chem. Phys.* **1999**, *110*, 9457–9462.
- (9) Raptis, R. G.; Fackler, J. P., Jr.; Murray, H. H.; Porter, L. C. *Inorg. Chem.* **1989**, *28*, 4059–4061.
- (10) Schwerdtfeger, P.; Dolg, M.; Schwarz, W. H. E.; Bowmaker, G. A.; Boyd, P. D. W. *J. Chem. Phys.* **1989**, *91*, 1762–1774.
- (11) Dirac, P. A. M.: *The Principles of Quantum Mechanics*, 4th ed.; Clarendon Press: Oxford, U. K., 1958; Chapter XI.
- (12) Visscher, L.; Jensen, H. J. A.; Saue, T.; Bast, R.; Dubillard, S.; Dyal, K. G.; Ekström, U.; Eliav, E.; Fleig, T.; Gomes, A. S. P.; Helgaker, T. U.; Henriksson, J.; Iliaš, M.; Jacob, C. R.; Knecht, S.; Norman, P.; Olsen, J.; Pernpointner, M.; Ruud, K.; Salek, P.; Sikkema, J. *DIRAC08*; Syddansk Universitet: Odense, Denmark, 2008. <http://dirac.chem.sdu.dk> (accessed Aug 20, 2010).
- (13) Douglas, M.; Kroll, N. M. *Ann. Phys.* **1974**, *82*, 89–155.
- (14) Hess, B. A. *Phys. Rev A* **1985**, *32*, 756–763.
- (15) Wolf, A.; Reiher, M.; Hess, B. A. *J. Chem. Phys.* **2002**, *117*, 9215–9226.
- (16) Reiher, M.; Wolf, A. *Relativistic Quantum Chemistry*; Wiley-VCH, Weinheim, Germany, 2009.
- (17) Dunning, T. H., Jr.; Hay, P. J. In *Modern Theoretical Chemistry*; Schaeffer, H. F., III, Ed.; Plenum Press: New York, 1976; Vol. 3, p 1.
- (18) Hay, P. J.; Wadt, W. R. *J. Chem. Phys.* **1985**, *82*, 299–310.
- (19) Stevens, W.; Basch, H.; Kraus, J. *J. Chem. Phys.* **1984**, *81*, 6026–6033.
- (20) Cundari, T. R.; Stevens, W. *J. Chem. Phys.* **1993**, *98*, 5555–5565.
- (21) Onoe, J.; Nakamatsu, H.; Mukayama, T.; Sekine, R.; Adachi, H.; Takeuchi, K. *J. Phys. Soc. Jpn.* **1996**, *65*, 2459–2462.
- (22) *J. Comput. Chem.* **2002**, vol. 23 (special issue).
- (23) Antschbach, J.; Siekierski, S.; Seth, M.; Schwerdtfeger, P. *J. Comput. Chem.* **2002**, *23*, 804–812.
- (24) Schwartz, H. *Angew. Chem., Int. Ed.* **2003**, *42*, 4442–4454.
- (25) Eickerling, G.; Mastalerz, R.; Herz, V.; Scherer, W.; Himmel, H.-J.; Reiher, M. *J. Chem. Theory Comput.* **2007**, *3*, 2182–2197.

- (26) Garin, J.; Toste, F. D. *Nature* **2007**, *446*, 395–403.
- (27) Iliáš, M.; Kellö, V.; Urban, M. *Acta Phys. Slov.* **2010**, *66*, 259–391.
- (28) Moncho, S.; Autsbach, J. *J. Chem. Theory Comput.* **2010**, *6*, 223–234.
- (29) Lein, M.; Rudolph, M.; Hashimi, S. K.; Schwedrtfeger, P. *Organometallics* **2010**, *29*, 2206–2210.
- (30) Odoh, S. O.; Schreckenbach, G. *J. Phys. Chem. A* **2010**, *114*, 1957–1963.
- (31) Cotton, F. A. *J. Mol. Struct.* **1980**, *59*, 97–108.
- (32) Mortola, A.; Moskowitz, J. W.; Rosch, N.; Cowman, C. D.; Gray, H. B. *Chem. Phys. Lett.* **1975**, *32*, 283–286.
- (33) Hay, P. J. *J. Am. Chem. Soc.* **1982**, *104*, 7007–7017.
- (34) Smith, D. C.; Goddard, W. A., III *J. Am. Chem. Soc.* **1987**, *109*, 5580–5583.
- (35) Blaudeau, J. P.; Roos, R. B.; Pitzer, R. M.; Mougenot, P.; Benard, M. *J. Phys. Chem.* **1994**, *98*, 7123–7127.
- (36) Wang, X.-B.; Wang, L.-S. *J. Am. Chem. Soc.* **2000**, *122*, 2096–2100.
- (37) Gagliardi, L.; Roos, B. O. *Inorg. Chem.* **2003**, *42*, 1599–1603.
- (38) Henandez-Avecedo, L.; Arratia-Perez, R. *J. Chil. Chem. Soc.* **2004**, *49*, 361–365.
- (39) Saito, K.; Nakao, Y.; Sato, H.; Sakaki, S. *J. Phys. Chem. A* **2006**, *110*, 9710–9717.
- (40) Ponec, R.; Yuzhakov, G. *Theor. Chem. Acc.* **2007**, *118*, 791–797.
- (41) Cavigliasso, G.; Kaltsoyannis, N. *Inorg. Chem.* **2007**, *46*, 3557–3565.
- (42) Krapp, A.; Lein, M.; Frenking, G. *Theor. Chem. Acc.* **2008**, *120*, 313–320.
- (43) Poineau, F.; Gagliardi, L.; Forster, P. M.; Sattelberger, A. P.; Czerwinski, K. R. *Dalton Trans.* **2009**, 5954–5959.
- (44) Ponec, R. *J. Math. Chem.* **1997**, *21*, 323–333.
- (45) Ponec, R. *J. Math. Chem.* **1998**, *23*, 85–103.
- (46) Ponec, R.; Duben, A. *J. Comput. Chem.* **1999**, *8*, 760–771.
- (47) Ponec, R.; Yuzhakov, G.; Carbo-Dorca, R. *J. Comput. Chem.* **2003**, *24*, 1829–1838.
- (48) Ponec, R.; Yuzhakov, G.; Girones, X.; Frenking, G. *Organometallics* **2004**, *23*, 1790–1796.
- (49) Ponec, R.; Yuzhakov, G.; Sundberg, M. *J. Comput. Chem.* **2005**, *26*, 447–454.
- (50) Ponec, R.; Feixas, F. *J. Phys. Chem. A* **2009**, *113*, 8394–8340.
- (51) McWeeny, R. *Rev. Mod. Phys.* **1960**, *32*, 335–369.
- (52) Bader, R. F. W. *Atoms in Molecules. A Quantum Theory*; Clarendon Press: Oxford, U. K., 1994.
- (53) Cioslowski, J. *Int. J. Quantum Chem.* **1990**, *S24*, 15–28.
- (54) Ponec, R.; Cooper, D. L. *Faraday Discuss.* **2007**, *135*, 31–42.
- (55) Ponec, R.; Cooper, D. L. *J. Phys. Chem. A* **2007**, *111*, 11294–11301.
- (56) Hohenberg, P.; Kohn, W. *Phys. Rev. B* **1964**, *136*, 864–871.
- (57) Kohn, W.; Sham, J. *Phys. Rev. A* **1985**, *140*, 1133–1138.
- (58) Schultz, N. E.; Zhao, Y.; Truhlar, D. G. *J. Phys. Chem A* **2005**, *109*, 4388–4403.
- (59) Vyboishchikov, S. F.; Sierralta, A.; Frenking, G. *J. Comput. Chem.* **1996**, *18*, 416–429.
- (60) Bo, C.; Costas, M.; Poblet, J. M. *J. Phys. Chem.* **1995**, *99*, 5914–5921.
- (61) Lin, Z.; Bytheway, I. *Inorg. Chem.* **1996**, *35*, 594–603.
- (62) Ponec, R.; Gatti, C. *Inorg. Chem.* **2009**, *48*, 11204–11031.
- (63) Dyall, K. G. *Theor. Chem. Acc.* **2004**, *112*, 403–409; available at <http://dirac.chem.sdu.dk> (accessed Aug 20, 2010).
- (64) Woon, D. E.; Dunning, T. H., Jr. *J. Chem. Phys.* **1993**, *98*, 1358–1371.
- (65) de Jong, W. A.; Harrison, R. J.; Dixon, D. A. *J. Chem. Phys.* **2001**, *114*, 48–53.
- (66) Frisch, M. J.; Trucks, G. W.; Schlegel, H. B.; Scuseria, G. E.; Robb, M. A.; Cheeseman, J. R.; Montgomery, J. A., Jr.; Vreven, T.; Kudin, K. N.; Burant, J. C.; Millam, J. M.; Iyengar, S. S.; Tomasi, J.; Barone, V.; Mennucci, B.; Cossi, M.; Scalmani, G.; Rega, N.; Petersson, G. A.; Nakatsuji, H.; Hada, M.; Ehara, M.; Toyota, K.; Fukuda, R.; Hasegawa, J.; Ishida, M.; Nakajima, T.; Honda, Y.; Kitao, O.; Nakai, H.; Klene, M.; Li, X.; Knox, J. E.; Hratchian, H. P.; Cross, J. B.; Adamo, C.; Jaramillo, J.; Gomperts, R.; Stratmann, R. E.; Yazyev, O.; Austin, A. J.; Cammi, R.; Pomelli, C.; Ochterski, J. W.; Ayala, P. Y.; Morokuma, K.; Voth, G. A.; Salvador, P.; Dannenberg, J. J.; Zakrzewski, V. G.; Dapprich, S.; Daniels, A. D.; Strain, M. C.; Farkas, O.; Malick, D. K.; Rabuck, A. D.; Raghavachari, K.; Foresman, J. B.; Ortiz, J. V.; Cui, Q.; Baboul, A. G.; Clifford, S.; Cioslowski, J.; Stefanov, B. B.; Liu, G.; Liashenko, A.; Piskorz, P.; Komaromi, I.; Martin, R. L.; Fox, D. J.; Keith, T.; Al-Laham, M. A.; Peng, C. Y.; Nanayakkara, A.; Challacombe, M.; Gill, P. M. W.; Johnson, B.; Chen, W.; Wong, M. W.; Gonzalez, C.; Pople, J. A. *Gaussian03*, revision C.02; Gaussian, Inc.: Wallingford, CT, 2004.
- (67) PROAIM, version 94, rev. B: Biegler, K. F. W.; Bader, R. F. W.; Tang, T. *J. Comput. Chem.* **1982**, *13*, 317–328.
- (68) AIMAll; Keith, T. A.; TK Gristmill Software: 1997. aim.tkgristmill.com (accessed Sep 2010).
- (69) Mayer, I. *Chem. Phys. Lett.* **1983**, *97*, 270–274.
- (70) Wiberg, K. *Tetrahedron* **1968**, *24*, 1083–1096.
- (71) Bader, R. F. W.; Stephens, M. E. *J. Am. Chem. Soc.* **1975**, *97*, 7391–7397.
- (72) Fradera, X.; Austin, M.; Bader, R. F. W. *J. Phys. Chem. A* **1999**, *103*, 304–314.
- (73) Jensen, F. *Introduction to Computational Chemistry*; John Wiley: Chichester, U. K., 2001; p 218.
- (74) Cotton, F. A.; Walton, R. A. *Multiple bonds between metal atoms*, 2nd ed.; Clarendon Press: Oxford, U. K., 1993.
- (75) Kuznetsov, V. G.; Kuzmin, P. A. *Zh. Struct. Khim.* **1963**, *4*, 55–62.
- (76) Ehlers, A. W.; Bohme, M.; Dapprich, S.; Gobbi, A.; Hollwarth, A.; Jonas, V.; Kohler, K. F.; Stegmann, R.; Veldkamp, A.; Frenking, G. *Chem. Phys. Lett.* **1993**, *208*, 111–114.